Mediterranean Archaeology and Archaeometry, Vol. 19, No 1, (2019), pp. 41-60
Open Access. Online & Print.

www.maajournal.com

DOI: 10.5281/zenodo.2585970

EVALUATION OF MALLORCA CATHEDRAL SEISMIC BEHAVIOR USING DIFFERENT ANALYSIS TECHNIQUES

Ahmed Elyamani*[1], Pere Roca[2], Oriol Caselles[2] and Jaime Clapes[2]

[1]Archaeological Conservation Department, Cairo University, Giza, Egypt
[2]Department of Civil and Environmental Engineering, Technical University of Catalonia, Barcelona, Spain

Received: 15/09/2018
Accepted: 11/02/2019
**Corresponding author: Ahmed Elyamani (a_elyamani@cu.edu.eg)*

ABSTRACT

The paper discusses the seismic assessment of Mallorca cathedral in Spain. This cathedral is an audacious Gothic structure built on the island of Mallorca during 14th-16th centuries, characterized by its large dimensions and slender structural members. For that purpose, different analysis methods were used. A 3D Finite Element (FE) model of the cathedral was created and then updated based on in-situ dynamic identification tests. Nonlinear static (pushover) analysis was firstly carried out applying the seismic loads in the longitudinal and transversal directions of the cathedral considering both positive and negative signs. The pushover results were compared with the results of the kinematic limit analysis as a way to cross check the seismic safety assessment. Although for such a large historical structure, the nonlinear time-history (dynamic) analysis requires a very high computer effort, an attempt to perform this type of advanced analysis was carried out.

KEYWORDS: Seismic assessment, Mallorca cathedral, pushover analysis, non-linear dynamic analysis, limit analysis

1. INTRODUCTION

Historical structures are very prone to earthquakes risks because they were not designed to sustain such lateral loading. Along the history, earthquakes in many countries rich with historical structures have resulted in catastrophic loss of many masterpieces of human architectural heritage. After L'Aquila earthquake (Italy) in 2009 the inspections carried out revealed that more than 50% of the cultural heritage buildings were in critical conditions and could not be used (Dolce, 2009). Due to the earthquake of Lisbon 1755 (Portugal), the two thirds of the city became uninhabitable, and about 35 churches, 65 convents, 33 palaces, the Royal library, the Patriarchal Palace and the Arsenal were ruined (Pereira, 2009).

Obviously, historical structures need to be seismically assessed and protected in order to ascertain its survival in the long term. In specific for large historical masonry structures, even when they are located in low to moderate seismic intensity zones, their vulnerability is of concern because of their extraordinary dimensions and, in some cases, their audacious structural design characterized by long span roofing elements and very slender vertical supporting elements.

The limited information about the different aspects of a historical structure under assessment is a main problem always faced. Information such as construction history, used construction techniques, collapses due to previous seismic events are often difficult to gather with certainty. A successful assessment approach should be based on combining and making use of the different investigation activities that may increase the level of knowledge about the historical structure to reduce the effect of such missed data. These activities include the historical investigation, the inspection (including laboratory and in-situ experiments), the monitoring and the structural analysis, among other possibilities (Elyamani and Roca, 2018a). These activities are used for gathering sufficient information about the assessed structure which may significantly contribute to design a minimal intervention and avoid unnecessary strengthening operations.

Currently, the usage of numerical models to understand and assess the structural safety of historical structures is gaining increasing interest (Elyamani et al, 2018b; El-Derby and Elyamani, 2016; Elyamani 2009, 2016& 2018). However, these models need a significant amount of information for their preparation. In addition, the models have to be validated, at the global level, by comparison with experimental evidence. This validation can be carried out by comparing the predictions of the model with results obtained related to the performance of the structure under known mechanical or environmental actions. This process is called numerical model updating. Afterwards, the updated model is used in the seismic analysis. In this step, different approaches may be used. The two most common techniques are nonlinear static analysis and nonlinear dynamic analysis, being the former is more widely used than the latter. To evaluate the structural performance of the assessed historical structure, simple methods like the N2 and the capacity spectrum could be utilized. Based on this evaluation, any necessary strengthening intervention could be proposed. The updated numerical model could be used as a virtual laboratory in which the proposed intervention could be simulated to reveal its adequacy and efficiency before any real implementation (Elyamani & Roca, 2018b).

This paper discusses the seismic assessment of Mallorca cathedral (Spain) using different analysis techniques. The cathedral is one of the largest historical masonry structures worldwide and dating back to the middle ages. Nonlinear static (pushover) analysis was firstly carried out. Then, the numerical results were compared with the results of the kinematic limit analysis as a way to cross check the seismic safety assessment. Although for such a large historical structure, the nonlinear time-history (dynamic) analysis seemed to be very time consuming, an attempt to perform this type of advanced analysis was carried out.

2. MALLORCA CATHEDRAL DESCRIPTION

Mallorca Cathedral is composed by three different bodies (Figure 1); those are the small apse (part A); a choir built in the shape of a single nave Gothic construction (part B) and the main nave (part C) which constitutes the main body of the building. The construction started around the year 1300. Parts A & B were completed around the years 1311 and 1370, respectively. The imposing main large nave and the west facade were completed by the year 1601 (Domenge, 1999).

The main nave is composed of a central nave and two lateral naves surrounded by a series of lateral chapels constructed between the buttresses. The central nave spans 19.9m and reaches a height of 43.9m at the vaults' keystone. The two lateral naves span 8.72m each and reach 29.4m at the vaults' keystone. The naves are supported on octagonal piers with a circumscribed diameter of 1.6 and 1.7m and a height of 22.7 m to the springing of the vaults. More details about the cathedral can be found at Elyamani and Roca (2018), Caselles et al. (2018, 2012) and Elyamani et al. (2012, 2018a).

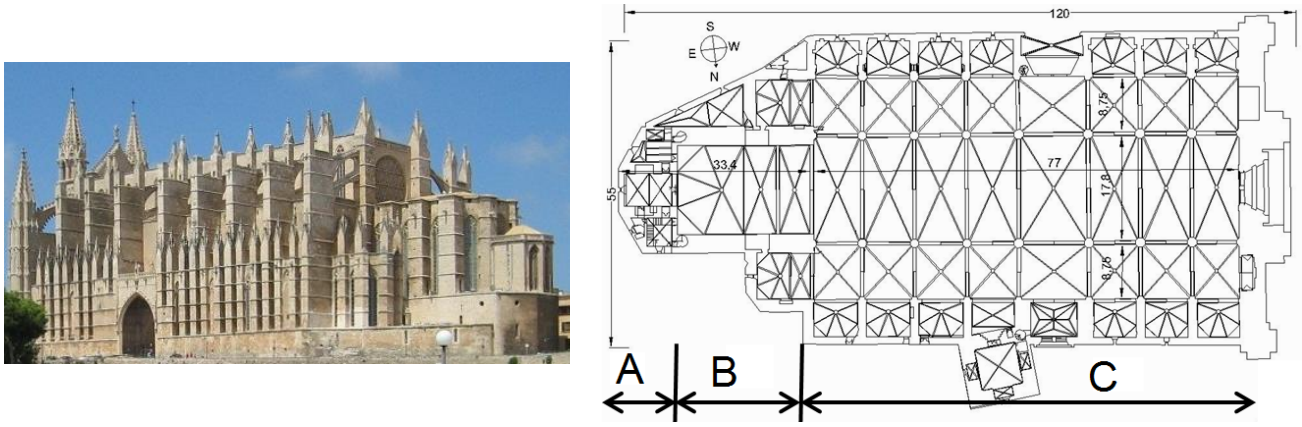

Figure 1. General view of Mallorca cathedral showing south facade and apse (left) and plan view (right).

3. PUSHOVER ANALYSIS

The FE model of the cathedral was built in DIANA FE code (Martinez, 2007). Vaults were modeled using T15SH elements (three-node triangular iso-parametric curved shells) and the rest of the cathedral was modeled using TE12L elements (four-node three-side iso-parametric solid pyramid). The model included 149248 nodes and 491851 elements with 490789 degrees of freedom. The model was updated based on in-situ dynamic identification tests (Elyamani et al., 2017a, 2017b). The nonlinear tensile behavior of the masonry was modeled using smeared cracking (multi-directional fixed crack model) and the compressive behavior was modeled using isotropic plastic Drucker-Prager model. Four different materials were identified in the cathedral and their properties are summarized in Table 1. The indicated Young's moduli were determined through the aforementioned model updating.

A monotonically increasing horizontal load was applied under constant gravity load. The adopted horizontal load distribution was a uniform load proportional to the structural elements' masses. The cathedral was subjected to the seismic loads in the longitudinal (X) and the transversal (Y) directions considering both the positive and the negative sings (±X and ±Y). Four control points were selected in order to represent the load-displacement curves. These points are the center of gravity of the full cathedral (CG-cathedral), the center of gravity of the naves' roof (CG-roof), the point with the highest elevation (Top) which is located at the top of the gable of the west facade, and the point with the maximum displacement (Max-D) in the direction under consideration. In Figure 2 the obtained capacity curves for the four cases are shown. The horizontal axis represents the displacement under seismic action and the vertical axis represents the resisted lateral load as a percent of the cathedral own weight.

Table 1. Used properties of the different materials in the FE model for the seismic assessment.

structural elements	Density (kg/m³)	Young's Modulus (MPa)	Poisson's ratio	Compressive strength (MPa)	Ultimate crack strain (%)
Walls and vaults	2100	3816	0.2	2	0.40
Buttresses	2100	2700	0.2	2	0.43
Columns and flying arches	2400	15264	0.2	8	0.10
Filling over vaults	2000	1908	0.2	1	0.81

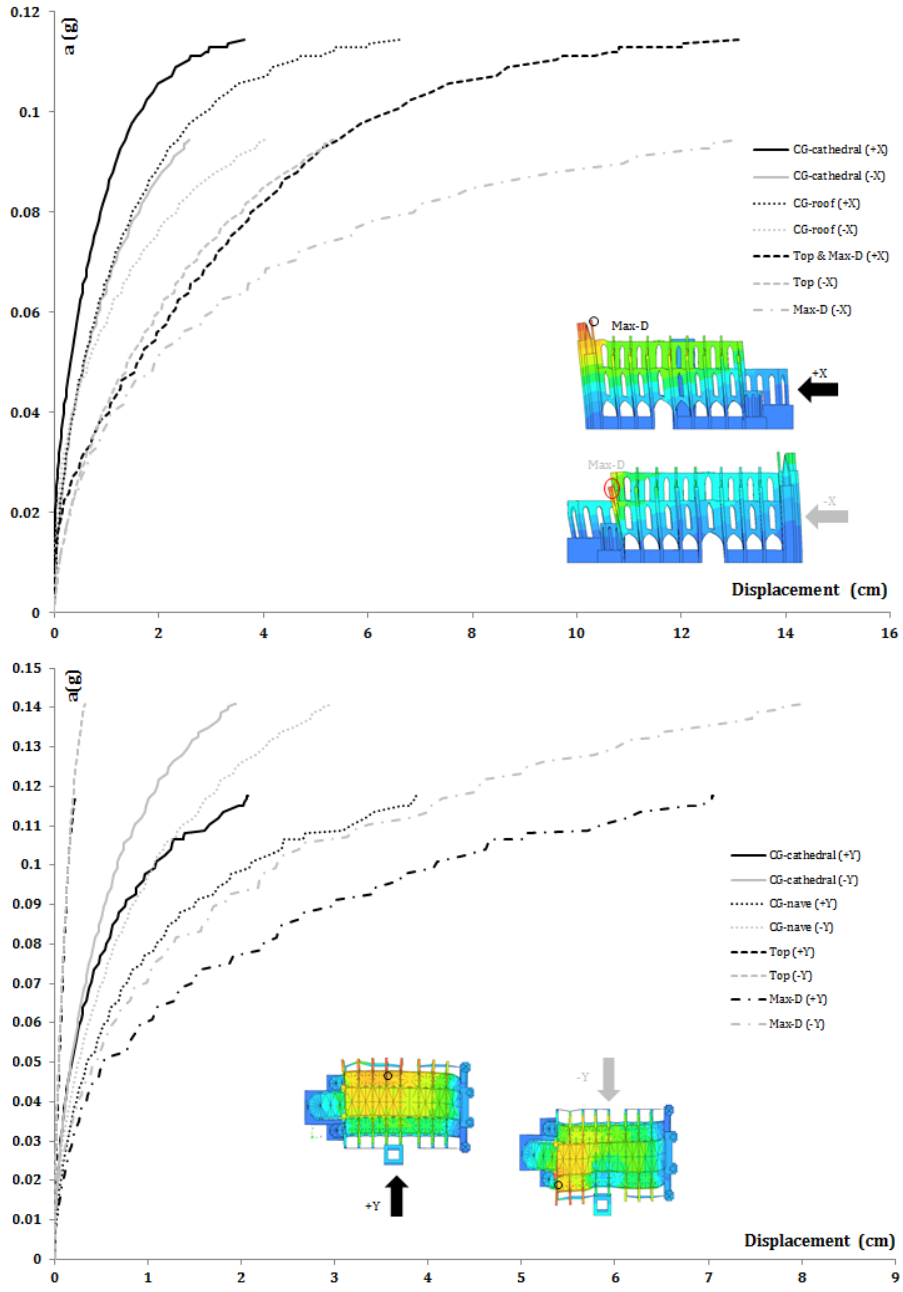

Figure 2. Capacity curve for the seismic analysis in (±X) direction (top) and (±Y) direction (bottom). The control point (Max-D) is shown in circle. "a" is the resultant base shear divided by the self-weight.

For the case of +X direction (Fig. 2, top), The point Top was found to be also the one with the highest displacement (Max-D). The behavior was linear up to a load value of about 0.040g. The collapse occurred at a load value of 0.114g due to the overturning of the west façade and consequent separation from the main nave (Figure 3, right). The –X direction (Fig. 2, top) showed the lowest capacity among the four considered directions. The attained capacity was only 0.095g and the collapse occurred due to the overturning of the east façade and consequent separation from the main nave (Figure 3, left).

In the +Y direction the cathedral showed a higher capacity (0.118g) than in the longitudinal direction (Fig. 2, bottom). The point Max-D was found to be at the top of the fifth flying arch counting from the west façade. As expected in masonry structures composed of arches, a series of disconnections (hinges) between structural parts could be noticed with the increase in the applied lateral load until reaching collapse (Figure 4, right). In –Y direction the resistance was the highest among all directions as can be seen in the capacity curve (Fig. 2, bottom). In this figure, the point Max-D was located at the top of the northern flying arch of the east façade. The obtained

capacity was 0.141g, about 20% more than +Y direction. The existence of the tower as a very stiff support near the middle of the structure was the reason for the higher capacity. The observed damage at collapse is shown in Figure 4 (left), similar to the previous case, a series of disconnections (hinges) were observed. More details can be checked at Elyamani et al (2017a).

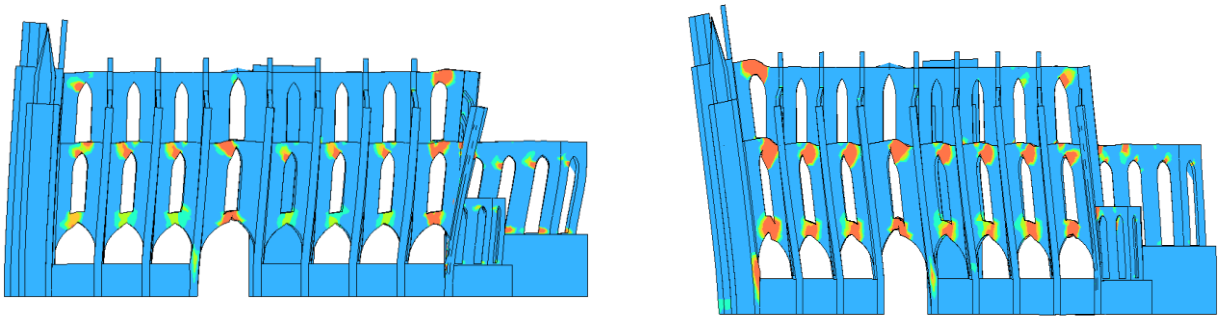

Figure 3. Damage pattern at collapse for case of –X (left) and +X (right).

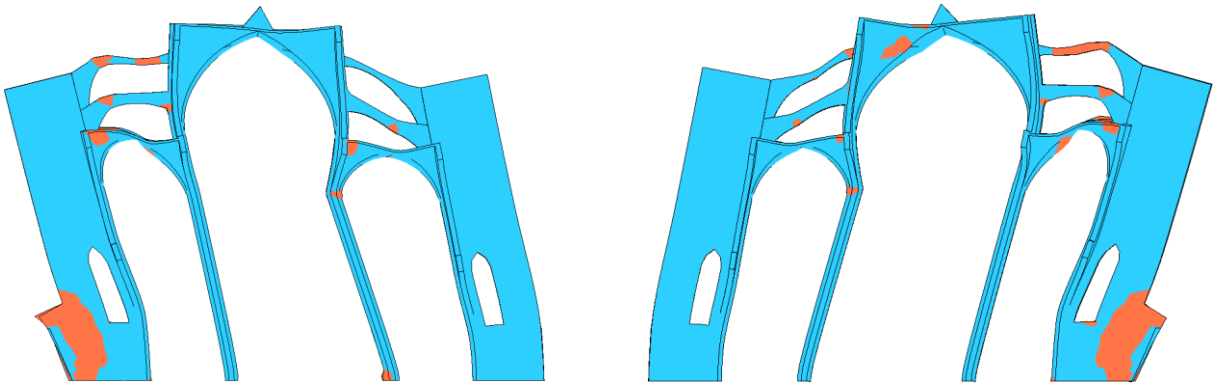

Figure 4. Damage pattern at collapse for case of –Y (left) and +Y (right).

4. KINEMATIC LIMIT ANALYSIS

Based on the collapse mechanisms found in the longitudinal direction by the pushover analysis, two collapse mechanisms were studied by the kinematic limit analysis. The overturning of the west and east facades was respectively considered in the +X and -X directions (Figure 5). The found capacities were 0.144g in the +X and 0.118g in the -X directions, respectively. These values are reasonably close to the capacities obtained by the pushover analysis.

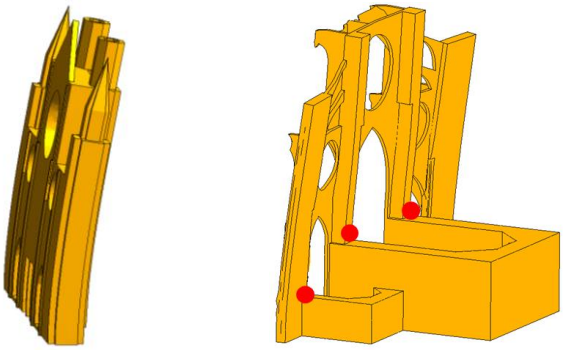

***Figure 5.** The west façade mechanism (left) and the east façade mechanism (right) (red circles are for hinges places).*

5. NON-LINEAR DYNAMIC ANALYSIS

5.1. Dynamic seismic loading

The EC-08 (CEN, 2004) gives two choices for the representation of the seismic action as time-history ground acceleration, the first is the use of artificial accelerograms and the second is the use of recorded accelerograms. The two approaches were used and in the following are presented and compared. For any of the two approaches, the derived accelerograms should be compatible with the site response spectrum. For this reason, the response spectra of the site of the cathedral were first determined as following.

For the case of the Spanish code (NCSE-02, 2002), it defines the seismic calculations acceleration (a_c) as:

$$a_c = S\,\rho\,a_b \qquad \text{Equation 1}$$

where: a_b is the basic seismic acceleration, the code value of 0,04g is used (mentioned in annex 1 for Palma de Mallorca zone); ρ is a coefficient considers the importance of the building and it considers tacitly the return period, ρ =1 and 1,3 for 475 and 975

years respectively; S is the coefficient of the soil amplification, it is calculated from one of the following three expressions:

For $\rho\, a_b \leq 0{,}1g$ $\quad S = \frac{C}{1{,}25}$ Equation 2

For $0{,}1g < \rho\, a_b < 0{,}4g$ $\quad S = \frac{C}{1{,}25} + 3{,}33\left(\rho \cdot \frac{a_b}{g} - 0{,}1\right)\left(1 - \frac{C}{1{,}25}\right)$ Equation 3

For $0{,}4g \leq \rho\, a_b$ $\quad S = 1{,}0$ Equation 4

In the above expressions C is the soil coefficient which equals 1,6 for the soil underneath the cathedral because it is considered a soil of type III with shear wave velocity between 200 and 400 m/s. More details about the cathedral's foundation soil were discussed in Elyamani (2015) and Elyamani and Roca (2018). S is calculated as 1,28 for the two considered return periods. Substituting the values of S, a_b and ρ in Equation 1, the acceleration a_c becomes equal to 0,051g and 0,067g for 475 and 975 years, respectively. Then to determine the response spectrum, a_c is multiplied by the normalized elastic spectrum of the code which has three branches defined by:

If $T < T_A$ $\quad \alpha\,(T) = 1 + 1{,}5 \cdot T/T_A$ Equation 5

If $T_A \leq T \leq T_B$ $\quad \alpha\,(T) = 2{,}5$ Equation 6

If $T > T_B$ $\quad \alpha\,(T) = K \cdot C/T$ Equation 7

where: α (T) is the value of the normalized response spectrum for 5% critical damping. T is the fundamental period of the structure in seconds. K is the coefficient of contribution, takes the value of 1 (annex 1 for the zone of Palma de Mallorca). T_A and T_B are calculated by means of the following equations: $T_A = K{\cdot}C/10 = 0{,}16$ s, and $T_A = K{\cdot}C/2{,}5 = 0{,}64$ s. The two response spectra are shown in Figure 6.

The Eurocode 8 (CEN, 2004) defines the horizontal response spectrum S_e (T) of the horizontal component of the seismic action by the following expressions:

$0 \leq T \leq T_B : S_e(T) = a_g \cdot S \cdot \left[1 + \frac{T}{T_B} \cdot (\eta \cdot 2{,}5 - 1)\right]$ Equation 8

$T_B \leq T \leq T_C : S_e(T) = a_g \cdot S \cdot \eta \cdot 2{,}5$ Equation 9

$T_C \leq T \leq T_D : S_e(T) = a_g \cdot S \cdot \eta \cdot 2{,}5 \frac{T_C}{T}$ Equation 10

$T_D \leq T \leq 4s : S_e(T) = a_g \cdot S \cdot \eta \cdot 2{,}5 \cdot \left[\frac{T_C T_D}{T^2}\right]$ Equation 11

Where: S_e (T) is the elastic response spectrum; T is the vibration period of a linear single-degree-of-freedom system; a_g is the design ground acceleration on type A ground ($a_g = \gamma_1 . a_{gR}$. γ_1 is the importance factor and a_{gR} is the reference peak ground acceleration on type A ground); T_B is the lower limit of the period of the constant spectral acceleration branch; T_c is the upper limit of the period of the constant spectral acceleration branch; T_D is the value defining the beginning of the constant displacement response range of the spectrum; S is the soil factor; η is the damping correction factor with a reference value of η = 1 for 5% viscous damping.

a_{gR} is 0,04g as defined in NCSE-02. The reference return period of the EC-08 is 475 years for which the γ_1 =1, so a_g =0,04g. For 975 years return period, γ_1 is calculated from the relation given in item 2.1(4) of the code: $\gamma_1 \sim (475/975)^{-1/3} = 1{,}27$, so a_g =0,051g. The soil type is B, so S = 1.2; T_B = 0.15 sec; T_C = 0.5 sec; and T_D = 2 sec. Figure 6 shows the two response spectra.

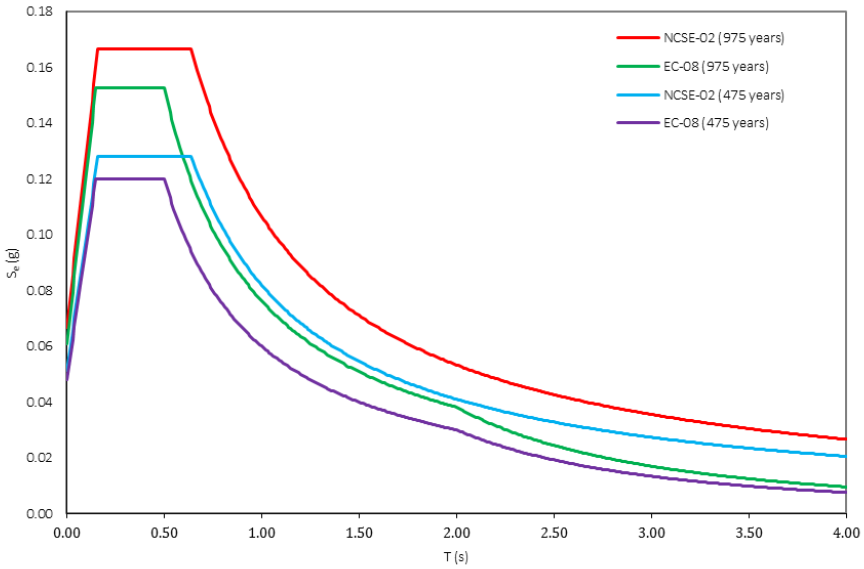

Figure 6. The elastic response spectrum Se (g) using the Eurocode 8 (EC8) and the Spanish code NCSE-02.

5.1.1. Artificial accelerograms

For Mallorca cathedral site, using the software SeismoArtif (SeismoArtif, 2016) seven artificial accelerograms were defined for each case of the response spectra of EC-08 (CEN, 2004) and NCSE-02 (NCSE-02, 2002) considering the two return periods of 475 and 975 years. The accelerograms were compatible with the spectra and were adapted to its frequency contents as required by the considered codes.

Figure 7 shows as an example one time-history for each code and return period. The four time-histories had the same time length about 7,5 seconds and they differed in the maximum PGA value and the significant time duration.

The comparison between the four cases in terms of the average PGA and the average significant duration of the seven records is shown in Figure 8. For the two considered return periods, the average PGA's of the time-histories of the NCSE-02 were higher than those of the EC-08. This was consistent with the spectra of the two codes (Figure 6). Regarding the significant duration, for all cases it changes in narrow range from about 4,05 to 4,27 seconds.

Figure 9 plots the average spectra of the seven accelerograms of the four cases with comparison with the codes spectra and the upper (+10%) and the lower (-10%) limits. As can be noticed for the four cases, the first branch of the spectrum was slightly higher than the upper limit, the second branch was aligned with the upper limit and the third branch was contained with the upper and lower limits.

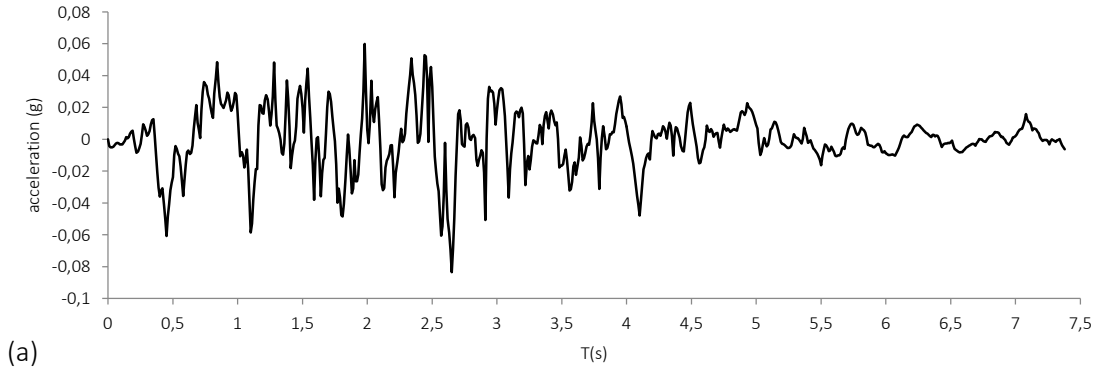

(a)

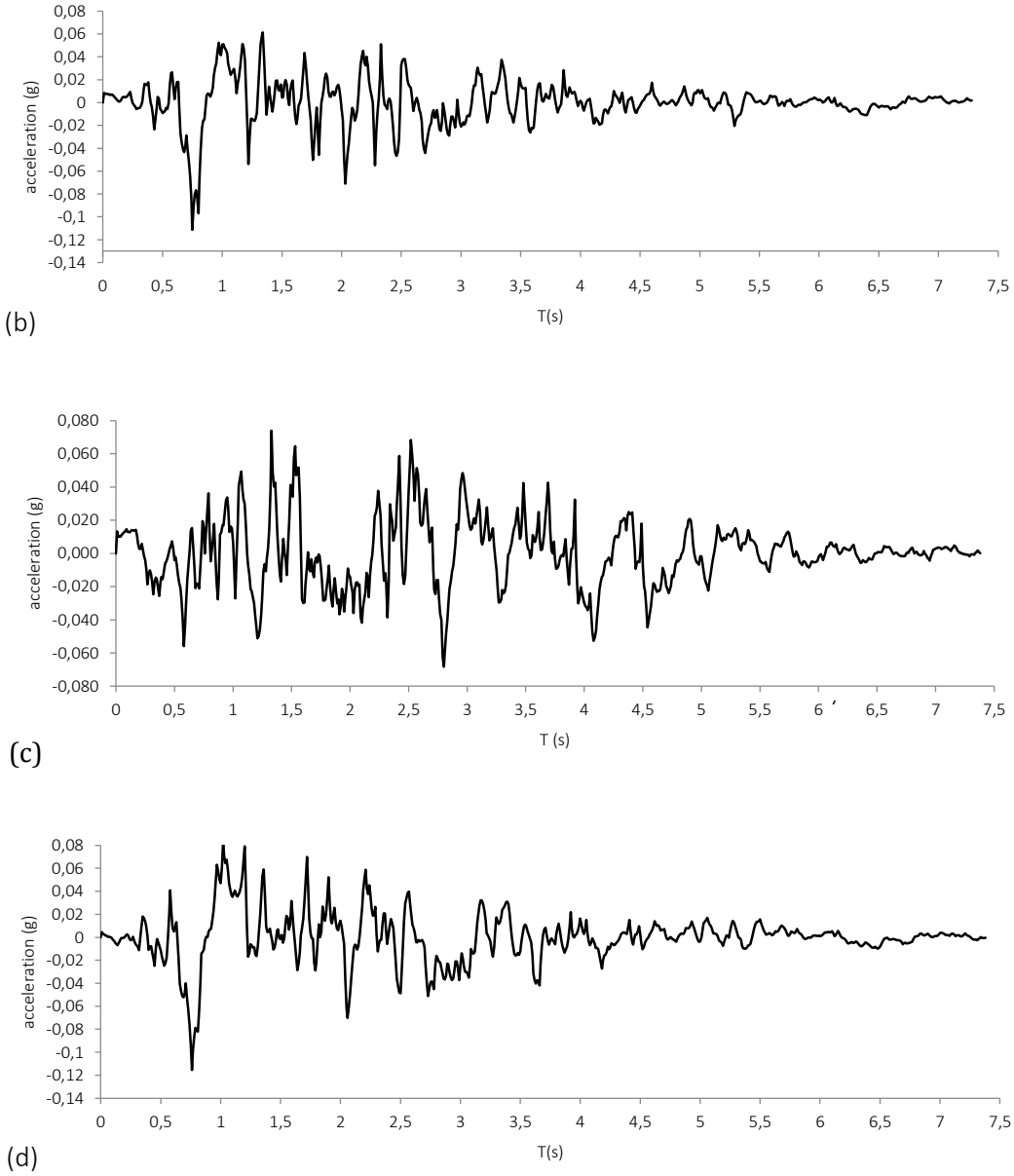

Figure 7. Artificial time-histories compatible with: (a) EC-08 (475 years); (b) EC-08 (975 years); (c) NCSE-02 (475 years); and (d) NCSE-02 (975 years).

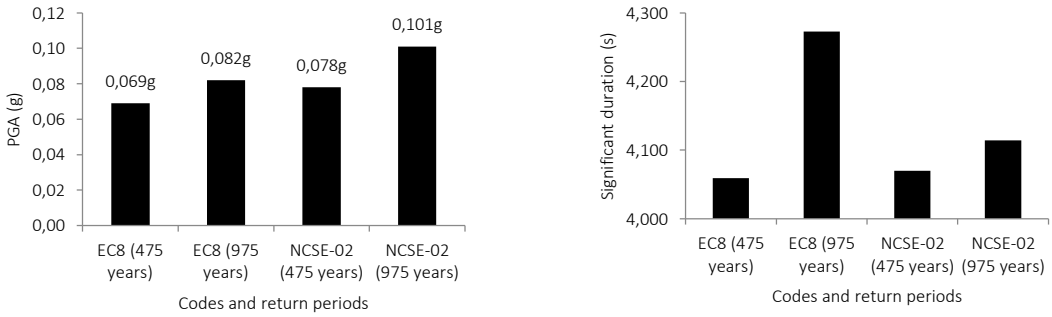

Figure 8. Comparison between artificial time-histories of considered codes and return periods: average PGA (left) and significant duration (right).

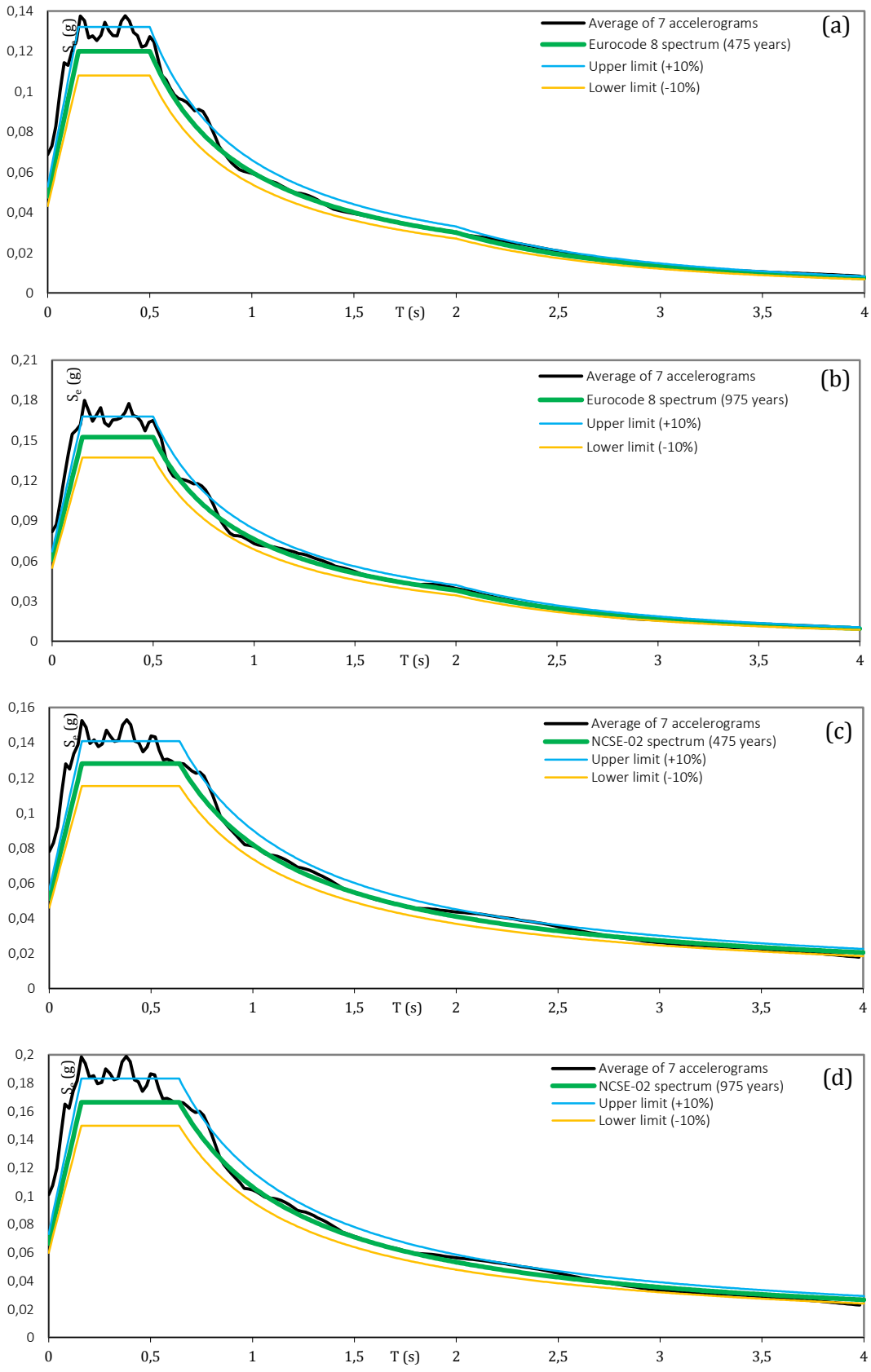

Figure 9. Spectra of the four cases using SeismoArtif : (a) Eurocode 8 (475 years); (b) Eurocode 8 (975 years); (c)NCSE-02 (475 years); and (d) NCSE-02 (975 years).

5.1.2. Real records accelerograms

The software REXEL v 3.5 (Iervolino et al. 2010) was used to find a compatible set of real records which their average spectrum is matched with the code spectrum. Each set was formed by seven real records. The records were selected from the European Strong-motion Database (http://www.isesd.cv.ic.ac.uk).

Table 2 reports the set of the seven earthquakes for each code and return period. The earthquake component and the station are mentioned in the table because for the same earthquake different PGA can be encountered depending on the direction of the earthquake component and the registration station. The highest PGA was not more than 0,101g which seemed reasonable for a low-to-moderate seismic intensity site of Mallorca Island.

A comparison between the averages PGA of the four combinations is depicted in Figure 10. As opposed to SeismoArtif, no information about the significant duration of the records was given by REXEL. Some examples of the real records are shown in Figure 11. The average spectra of the seven real records of the four cases in comparison with the codes spectra and the upper (+10%) and the lower (-10%) limits are plotted in Figure 12. For the two return periods of EC-08, the average spectra were within the limits or slightly higher than the upper limit. On the other side, for NCSE-02, the average spectra were slightly lower than the lower limit for periods more than 2 s and 2,5 s for 475 and 975 years, respectively. However, these spectra were still suitable since the periods of interest for Mallorca cathedral were from T=0,7 s or less, where 0,7 s was the period of the first mode.

Table 2. Details of the combination of earthquake records compatible with the spectrum of each code and return period.

Code (return period)	Earthquake name (component direction-station)	Date	M_w	PGA(g)
EC-08 (475)	Umbria Marche aftershock (y-ST228)	03/04/1998	5,1	0,046
	Friuli (x-ST15)	06/05/1976	6,5	0,052
	Izmit (y-ST574)	17/08/1999	7,6	0,042
	Izmit (y-ST2572)	17/08/1999	7,6	0,063
	Montenegro (y-ST70)	15/04/1979	6,9	0,058
	Montenegro (aftershock) (y-ST77)	24/05/1979	6,2	0,055
	Gulf of Akaba (y-ST2898)	22/11/1995	7,1	0,091
EC-08 (975)	Almiros aftershock (y-ST1300)	11/08/1980	5,2	0,072
	Izmit (x-ST766)	17/08/1999	7,6	0,086
	Ano Liosia (x-ST1141)	07/09/1999	6,0	0,085
	Ano Liosia (x-ST1255)	07/09/1999	6,0	0,087
	Friuli (aftershock) (x-ST28)	15/09/1976	6,0	0,066
	Manjil (x-ST190)	20/06/1990	7,4	0,068
	Ano Liosia (y-ST1257)	07/09/1999	6,0	0,086
NCSE-02 (475)	Almiros aftershock (x- ST1300)	11/08/1980	5,2	0,072
	Izmit (y- ST766)	17/08/1999	7,6	0,099
	Montenegro (x- ST63)	09/04/1979	5,4	0,071
	Ano Liosia (x- ST1255)	07/09/1999	6,0	0,087
	Friuli (x- ST14)	06/05/1976	6,5	0,064
	Paliouri (x- ST1329)	10/04/1994	5,1	0,062
	Izmit (y- ST779)	17/08/1999	7,6	0,076
NCSE-02 (975)	Izmit (x-ST766)	17/08/1999	7,6	0,086
	Ano Liosia (x-ST1141)	07/09/1999	6,0	0,085
	Patras (y-ST178)	22/12/1988	4,9	0,101
	Aigion (y-ST1331)	15/06/1995	6,5	0,093
	Ano Liosia (y-ST1101)	07/09/1999	6,0	0,109
	Umbria Marche aftershock (y-ST265)	14/10/1997	5,6	0,082
	Izmit (x-ST556)	17/08/1999	7,6	0,092

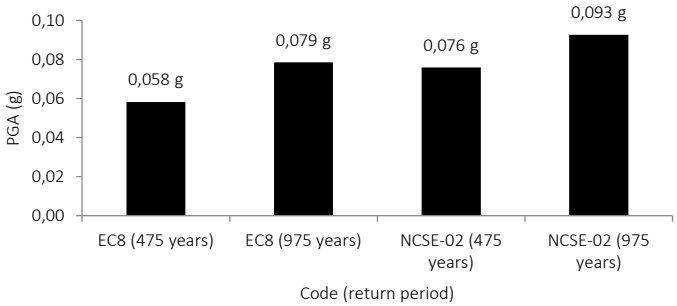

Figure 10. The average PGA of each combination of real records compatible with each code and return period.

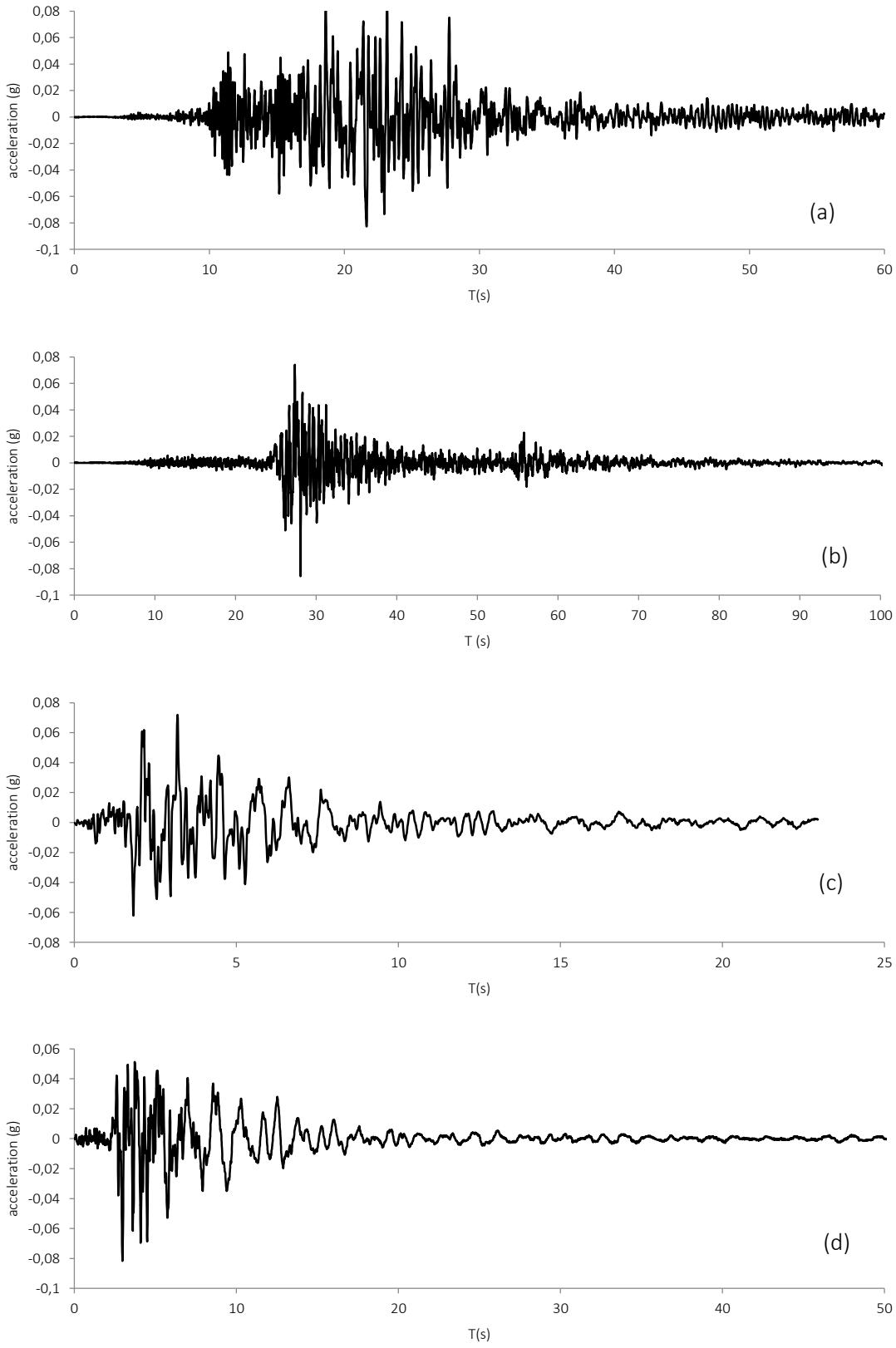

Figure 11. Examples of the real records mentioned in table 1.12 :(a) Gulf of Akaba (y-ST2898); (b) Izmit (x-ST766); (c) Almiros aftershock (x- ST1300); and (d) Umbria Marche aftershock (y-ST265).

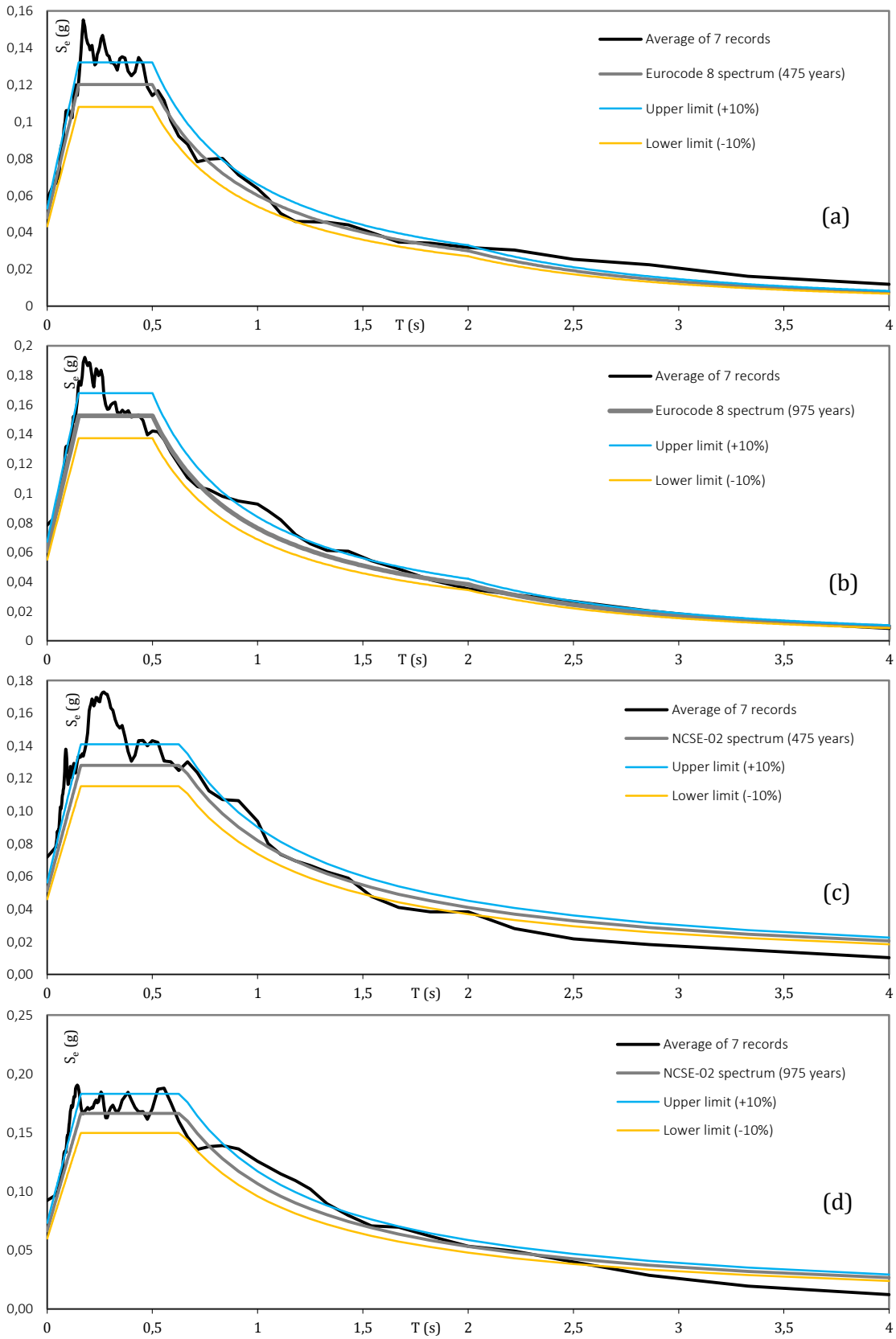

Figure 12. Spectra of the four cases using REXEL: (a) Eurocode 8 (475 years); (b) Eurocode 8 (975 years); (c) NCSE-02 (475 years); and (d) NCSE-02 (975 years).

5.1.3. Comparison between the artificial and the real records

A comparison between the average spectra of the artificial and the real records is shown in Figure 13. It can be seen that for the four cases considered, very near spectra were found. Also, when comparing the PGA (Figure 14) near values could be noticed.

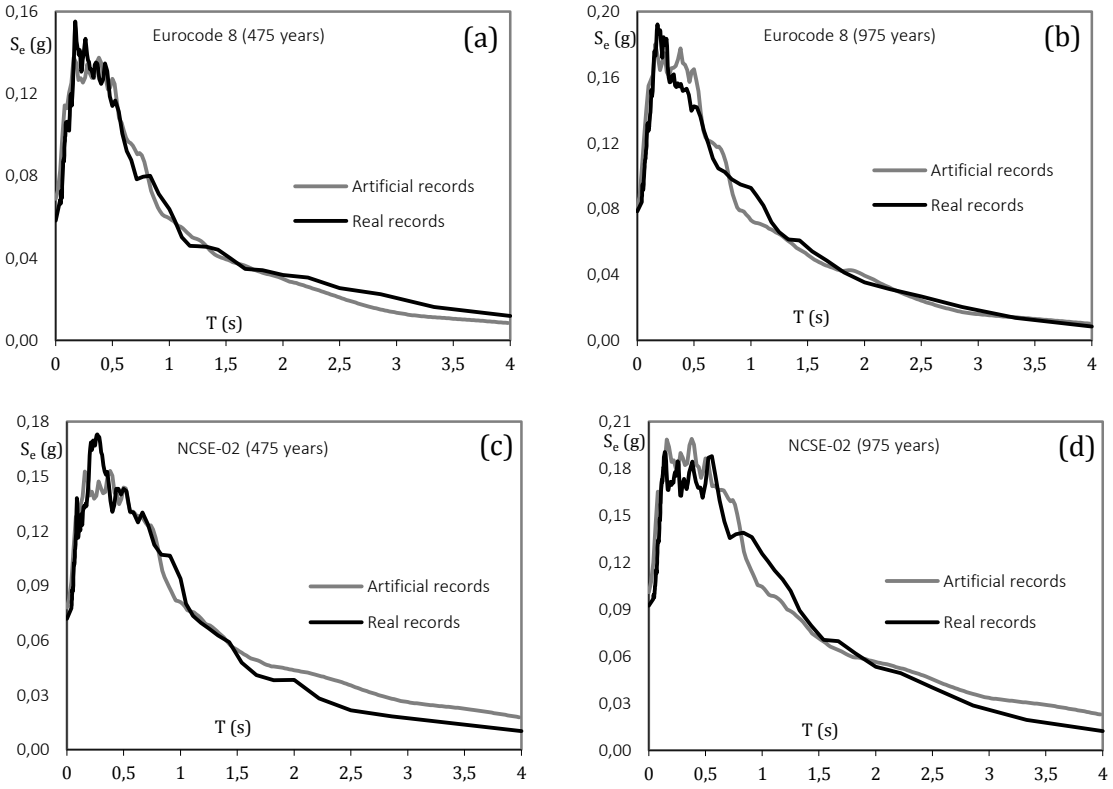

Figure 13. Comparing spectra of the artificial and the real records: (a) Eurocode 8 (475 years); (b) Eurocode 8 (975 years); (c) NCSE-02 (475 years); and (d) NCSE-02 (975 years).

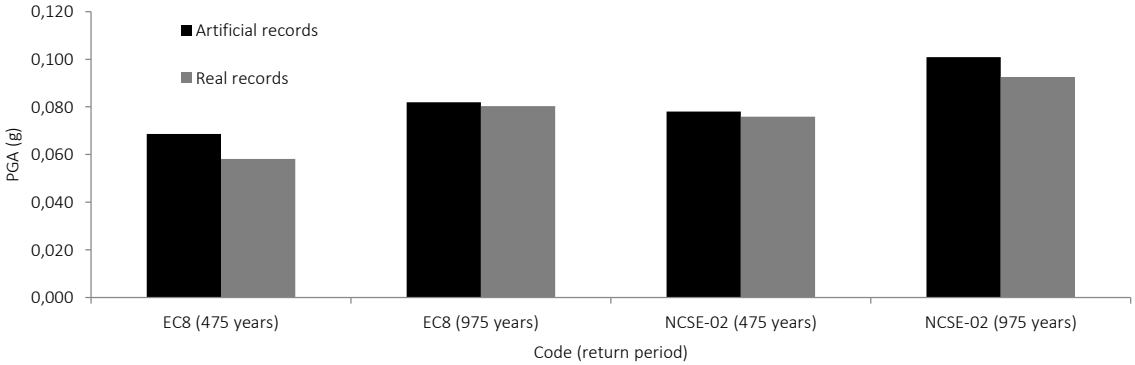

Figure 14. Comparison between the average PGA (g) of the artificial and the real records.

5.2. *Time step and damping model*

The analysis was carried out using one accelerogram only in one direction. The accelerogram in Figure 7-d was applied to the cathedral in the longitudinal direction (see results in section 5.3) and then in the transversal direction (see results in section 5.4). The time step Δt was adopted making reference to Newmark method (Newmark, 1959). When applying this method, the choice of the time step size (Δt) should satisfy the following two conditions:

(1) it is sufficiently small compared with the accelerogram duration (t_d)

$$\Delta t \ll t_d \qquad \text{Equation 12}$$

(2) to correctly reproduce the system response, preferably 20 time steps must be applied in the small period (T_i) of the highest mode

$$\Delta t \leq \frac{1}{20} T_i \qquad \text{Equation 13}$$

thus ensuring the correct computation of the contribution of high-frequency modes (DIANA, 2009). According to Eurocode 8 (CEN, 2004) enough number of modes should be taken into account to ensure correct consideration of all modes contributing significantly to the dynamic response. This condition is satisfied by considering a number of modes corresponding to a cumulative mass participation of at least 90% in relevant directions of the analysis.

Table 3 presents the number of modes and the corresponding cumulative mass participation calculated from the FE model of the cathedral. It was observed that considering 600 modes resulted in a cumulative mass participation of 89%, 100% in the longitudinal and the transversal directions, respectively, which satisfied the requirements of the Eurocode 8 (CEN, 2004). Thus, substituting T_{600} (0,0407 s) in Equation 13 gave Δt = 0,002 s. The applied accelerogram had t_d of 7,38 s, this resulted in a number of time steps =7,38/0,002= 3690 which was too much. Therefore, Δt of 0,01 s was considered and the number of the time steps was reduced to 738 (7,38/0,01). This meant that the highest considered T_i equaled 20×0,01=0,2 s. This period was the same as the one of the mode number 44. Considering 44 modes gave a cumulative mass participation of about 73% and 63% in the longitudinal and the transversal directions, respectively. Although the used Δt did not satisfy the Eurocode 8 requirements, it was less computational time demanding. In addition, Δt was small enough compared with the earthquake duration so it satisfied Equation 12. The previously discussed reasoning was based on that followed in the nonlinear dynamic analysis of St. George of the Latins church (Trujillo, 2009; Lourenço et al., 2012).

Table 3. The number of considered modes and the corresponding cumulative mass participation (%).

Direction	Number of considered modes						
	50	100	200	300	400	500	600
Longitudinal	70	73	78	82	87	88	89
Transversal	79	91	96	98	99	99	100

To introduce damping in the model, the Rayleigh damping model was used due to its mathematical simplicity. The Rayleigh damping (c) is defined as a combination of the mass (m) and the stiffness (k):

$$c = a_0 \cdot m + a_1 \cdot k \qquad \text{Equation 14}$$

where, a_0 and a_1 are the Rayleigh damping coefficients. These two coefficients can be determined from the damping ratios (ξ_i and ξ_j) and the angular frequencies (ω_i and ω_j) of the i^{th} and j^{th} modes as follows:

$$\frac{1}{2}\begin{bmatrix} 1/\omega_i & \omega_i \\ 1/\omega_j & \omega_j \end{bmatrix}\begin{Bmatrix} a_0 \\ a_1 \end{Bmatrix} = \begin{Bmatrix} \xi_i \\ \xi_j \end{Bmatrix} \qquad \text{Equation 15}$$

The damping (ξ_n) of any mode n^{th} with angular frequency (ω_n) can be determined as:

$$\xi_n = \frac{a_0}{2} \cdot \frac{1}{\omega_n} + \frac{a_1}{2} \cdot \omega_n \qquad \text{Equation 16}$$

When applying this procedure, the two modes (i^{th} and j^{th}) should be reasonably chosen such that the obtained values of a_0 and a_1 result in reasonable damping ratios for all the modes contributing in the dynamic behavior of the structure (Chopra, 2000).

The first mode was considered as the i^{th} mode, since it has a significant mass participation in the longitudinal direction (about 60%). The j^{th} mode was the mode number 44 as found from the previous calculations of Δt. Assuming a reasonable damping of 0,05 (Mendes, 2012; Cagnan, 2012; Peña et al., 2010), the Rayleigh coefficients were calculated as a_0=0,68858 and a_1=0,00253. Figure 15 shows the variation of Rayleigh damping along the natural frequencies of the cathedral. As seen, the damping is 0,05 or less in the range from 1,41 Hz (mode 1) to 4,92 Hz (mode 44) then values more than 0,05 can be noticed for the modes higher than 44.

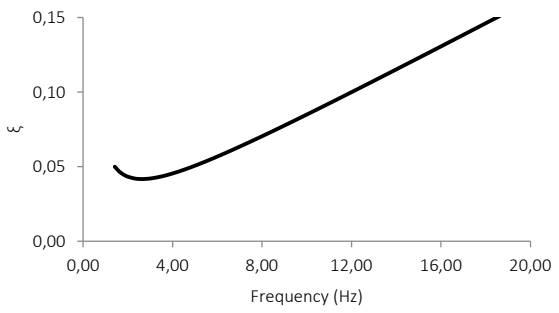

Figure 15. Distribution of Rayleigh damping along the cathedral modes.

5.3. *Analysis in the longitudinal direction*

The cathedral was able to resist the complete time history without collapse. The analysis lasted for 8 days and about 12 hours using a standard PC provided with Intel ® Core ™ i5 of 2.67 GHz and RAM of 8 GB. Regarding the displacement history in time, it was found that the points with the highest displacement were the same as found in the pushover analysis in ±X directions. In Figure 15 (top) the displacements' time histories of the control points previously considered in the pushover analysis are shown. The absolute maximum resisted load was 0,071g as can be noticed in Figure 15 (bottom) that shows the relation between the displacements of the control points and the seismic load multiplier (the horizontal reaction/the self-weight).

The damage at the two time steps of the maximum displacements (points "a" and "b" in Figure 15 (top)) are depicted in Figure 16 and compared with those obtained by the pushover analysis (at the same acceleration). It can be noticed that the damaged locations were the same as that found by the pushover analysis in ±X directions. However, less damage than in the pushover analysis could be noticed.

The displacements obtained from this analysis were compared with those obtained from the pushover analysis for the same direction and at the same applied acceleration, Table 4. It can be observed that the values of the deformations obtained from the pushover analysis were always much less than those obtained by the nonlinear dynamic analysis. Therefore, the nonlinear dynamic analysis produced less damage but larger deformation in the building. For a more comprehensive comparison, a larger number of accelerograms (at least seven) should be applied and the average displacements should be compared to the results of the pushover analysis as recommended by the Eurocode 8 (CEN, 2004).

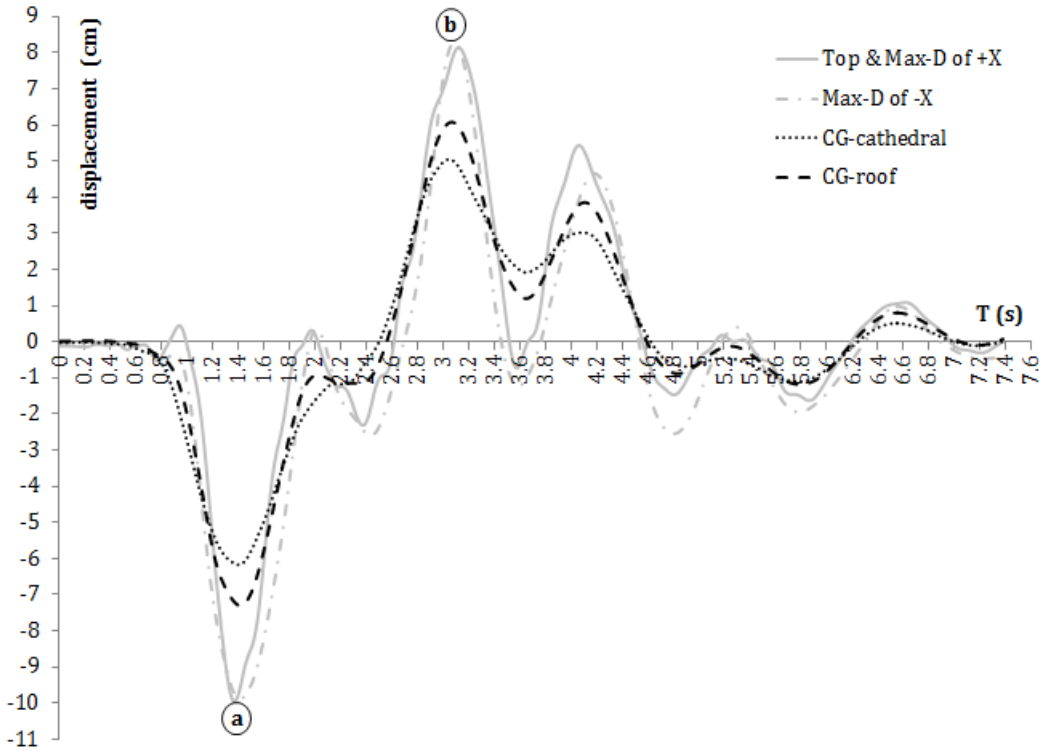

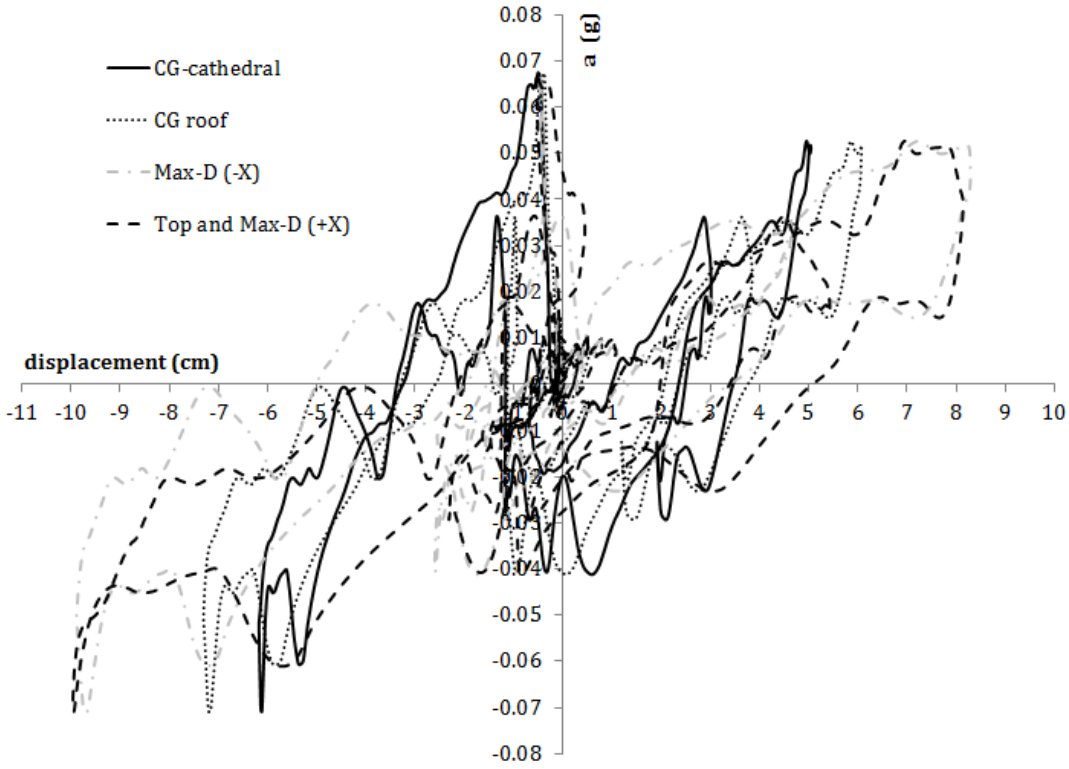

Figure 16. Time histories of the displacements of the considered control points (Top); relation between seismic load multiplier (a (g)) and displacements of the control points (bottom). Case of nonlinear dynamic analysis in the longitudinal direction of the cathedral.

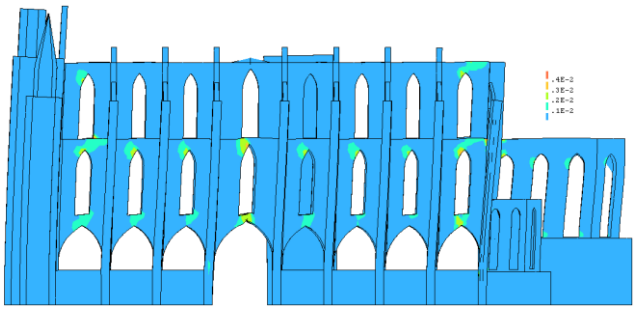

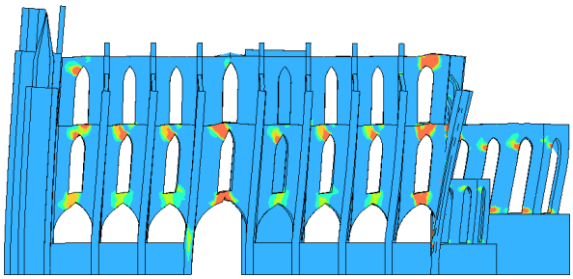

Damage pattern at the maximum negative displacement (point "a" in Figure 15-top).

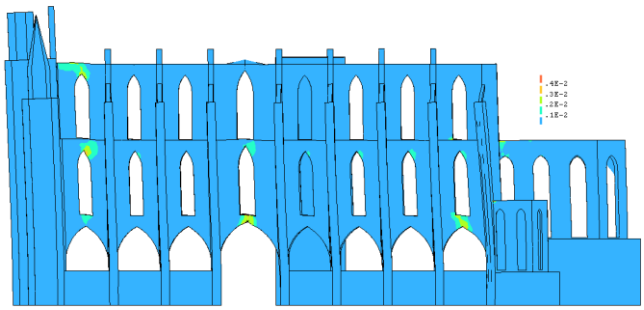

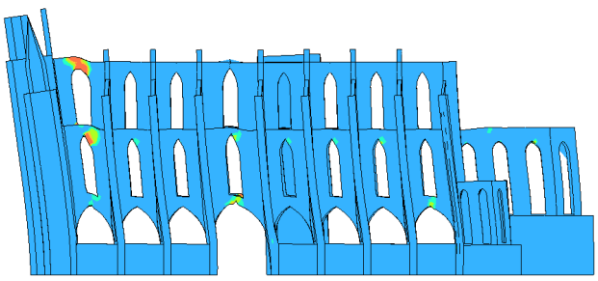

Damage pattern at the maximum positive displacement (point "b" in Figure 15-top).

Figure 17. Damage pattern in the typical resisting frame, nonlinear dynamic analysis (left) and pushover analysis at the same acceleration (right). Contour of maximum principal strain plotted on deformed mesh.

Table 4. Control points displacements from Nonlinear Dynamic Analyses (NDA) and corresponding pushover (±X & ±Y).

Case	Control point							
	CG-cathedral		CG-roof		Max-D		Top	
NDA longitudinal direction	Max (+)	Max (-)	Max (+)	Max (-)	Max (+)	Max (-)	Max (+)	Max (-)
	4.9	6.2	6.1	7.3	8.3	10.0	7.8	10.0
Corresponding Pushover (±X)	+X	-X	+X	-X	+X	-X	+X	-X
	0.3	1.2	0.6	1.6	1.7	4.6	1.7	2.7
NDA transversal direction	Max (+)	Max (-)	Max (+)	Max (-)	Max (+)	Max (-)	Max (+)	Max (-)
	4.4	5.5	4.9	6.2	5.7	6.6	4.2	4.4
Corresponding Pushover (±Y)	+Y	–Y	+Y	–Y	+Y	–Y	+Y	–Y
	0.1	0.3	0.1	0.5	0.2	1.0	0.0	0.1

5.4. *Analysis in the transversal direction*

The cathedral resisted the full accelerogram without collapse. The analysis lasted for 5 days and about 12 hours. Figure 18 (top) reports the time history of the different control points previously considered. Also in this analysis, the displacements found were larger than those obtained by the pushover analysis, Table 4. The same locations of hinges previously found by the pushover analysis were obtained by the nonlinear dynamic analysis with clearly less damage than the pushover cases in ±Y directions, Figure 19. As for the longitudinal direction, the nonlinear dynamic analysis produced larger deformation but less damage. Finally, Figure 18 (bottom) shows for some points the relation between the displacements and the seismic load multiplier.

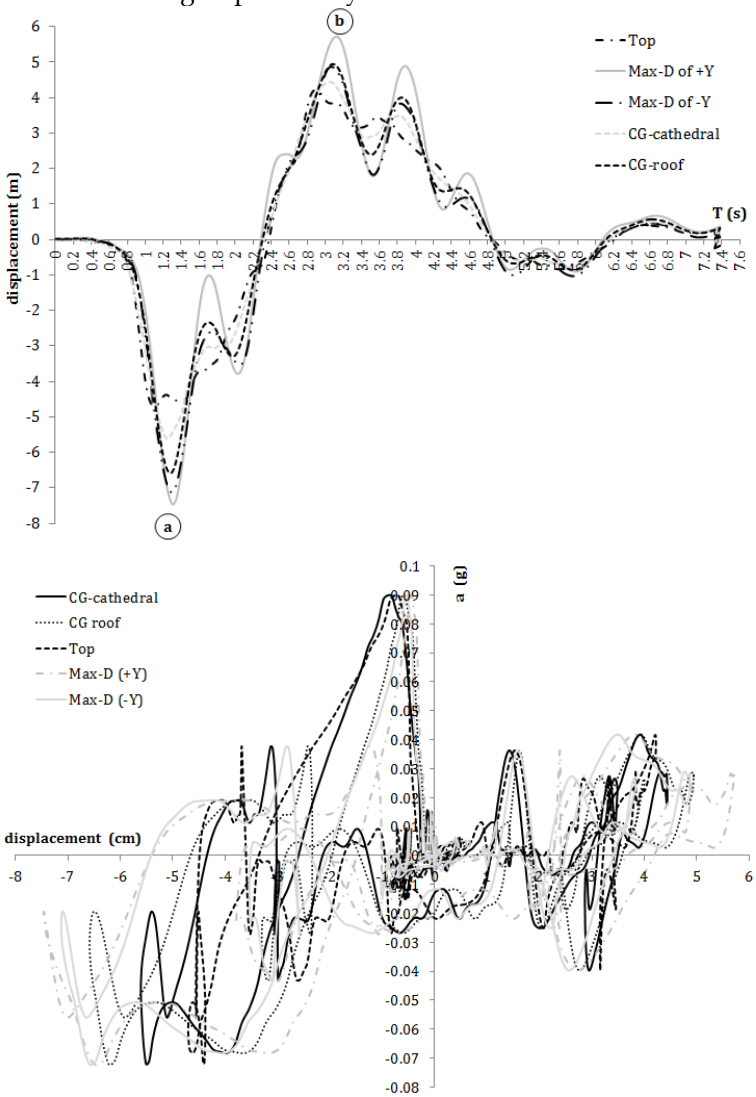

Figure 18. Time histories of the displacements of the considered control points (top); relation between seismic load multiplier (a (g)) and displacements of control points (bottom). Case of nonlinear dynamic analysis in the transversal direction of the cathedral.

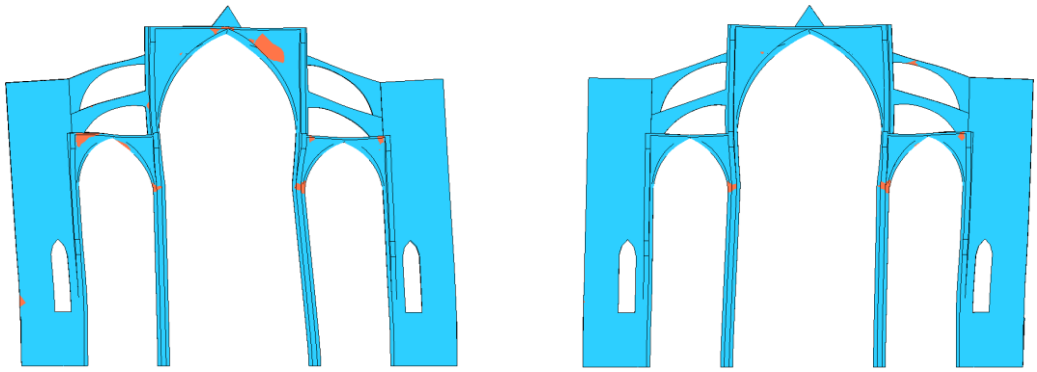

Figure 19. Damage pattern in a typical frame. Contour of maximum principal strain plotted on deformed mesh: (left) damage pattern at the maximum negative displacement, point "a" in Figure 18; (right) Damage pattern at the maximum positive displacement (point "b" in Figure 18).

6. CONCLUSIONS

The seismic analysis of Mallorca cathedral was carried out using three different analysis techniques, namely pushover analysis, kinematic limit analysis and nonlinear dynamic analysis. The cathedral showed different capacities depending on the direction of the applied seismic loads. The higher capacity was obtained for seismic loads applied in the transverse direction. In this direction, the buttresses, which represented the main seismic-resistant elements in the building, are loaded in their stiffer in-plane direction. The observed collapse mechanism for the seismic analysis in the longitudinal direction is the overturning of the east and west facades. For the analysis in the transversal direction, the collapse mechanism is determined by the generation of a number of hinges in the structure of the typical bay these hinges are developed in the flying arches, the arches and vaults of the naves, the top and bottom sections of the piers and the bottom sections of the buttresses. The nonlinear dynamic analysis predicted a similar collapse mechanism to that found with pushover analysis.

When comparing the pros and cons of each of the employed techniques, we found that the limit analysis is a simple technique; however, it needs some evidences to predict which failure mechanisms would be activated such as cracks observed in the structure or predicted by another analysis technique like the pushover. As well, it can hardly be used to predict the damage for moderate or service load levels not leading to a limit condition. It should be considered as a complementary tool when performing alternative numerical analyses. The nonlinear static analysis is less demanding in terms of time and computer effort when compared to the nonlinear dynamic analysis. It is a relatively simple structural analysis technique that aims at evaluating the expected performance of a structure under earthquakes by estimating its strength and deformation capacities. It accounts in an approximate manner for the redistribution of internal forces occurring when the structure is subjected to inertia forces that no longer can be resisted within the elastic range of the structural behavior. However, this technique has some limitations such as the inability to account for the progressive stiffness degradation; the invariant load patterns cannot account for the contributions of higher modes to the structural response; it may not detect some important deformation modes of the structure when subjected to severe earthquakes and it may exaggerate others; among others. The nonlinear dynamic analysis is very demanding in terms of time and computer effort. There is a dependency of the predicted behavior on the used input ground motion and damping ratio. For the latter, for instance, the displacements are expected to decrease when increasing the used damping ratio. Therefore, there is a need to carry out a sensitivity analysis on this factor to estimate the envelope of the behavior under different damping ratios.

ACKNOWLEDGEMENTS

This research has been carried out within the project "New Integrated Knowledge based approaches to the protection of cultural heritage from Earthquake-induced Risk-NIKER" funded by the European Commission (Grant Agreement n° 244123), whose assistance is gratefully acknowledged.

REFERENCES

Caselles, O., Clapes, J., Roca, P. and Elyamani, A., (2012) Approach to seismic behavior of Mallorca cathedral. *15th World Conference of Earthquake Engineering, 24-28 September 2012, Lisbon, Portugal.*

Caselles, O., Clapes, J., Elyamani, A., Lana, J., Segui, C., Martin, A. and Roca, P. (2018) Damage detection using Principal Component Analysis applied to temporal variation of natural frequencies. *16th European Conference on Earthquake Engineering, 18-21 June 2018, Thessaloniki, Greece.*

CEN (2004) Eurocode 8 - Design Provisions for Earthquake Resistance of Structures, Part 1.1: General rules, seismic actions and rules for buildings, European prestandards ENV 1998, European Committee for Standardization, Brussels.

Chopra, A. K. (2000). *Dynamic of structures – Theory and Applications to Earthquake Engineering*. Prentice Hall.

DIANA (2009) Diana 9.4, user's manual. The Netherlands: TNO Building and Construction Research. Available from www.diana.tno.nl.

Dolce, M. (2009). The Abruzzo earthquake: effects and mitigation measures. *Disaster prevention workshop*, Stockholm, Hasselbacken, 27-29 July 2009.

Domenge J (1999) *L'obra de la Seu. El process de construcció de la Catedral de Mallorca en el tres-cents*, Institu d'Estudis Balears, Palma de Mallorca (in Catalan).

Elyamani, A. and Roca, P. (2018) One century of studies for the preservation of one of the largest cathedrals worldwide: A review. *SCIENTIFIC CULTURE*, 4(2), pp.1-24. DOI: 10.5281/zenodo.1214557

Elyamani, A., Caselles O., Roca, P. and Clapes, J. (2018a) Integrated dynamic and thermography investigation of Mallorca Cathedral. *Mediterranean Archaeology & Archaeometry*, 18(1), pp.221-236. DOI: 10.5281/zenodo.1165360.

Elyamani, A., Roca, P., Caselles, O., and Clapes, J. (2017a) Seismic safety assessment of historical structures using updated numerical models: The case of Mallorca cathedral in Spain. *Engineering Failure Analysis*, Vol. 74, pp. 54-79. DOI: https://doi.org/10.1016/j.engfailanal.2016.12.017

Elyamani, A., Caselles, J.O., Roca, P and Clapes, J. (2017b) Dynamic investigation of a large historical cathedral. *Structural Control and Health Monitoring*, Vol. 24. DOI: 10.1002/stc.1885.

Elyamani, A., J. O. Caselles, J. Clapes, and P. Roca, (2012) Assessment of dynamic behavior of Mallorca cathedral, *8th International Conference of Structural Analysis of Historical Construction*, Wroclaw, Poland, 15-17 Oct. 2012.

Elyamani, A. (2015) Integrated monitoring and structural analysis strategies for the study of large historical construction. Application to Mallorca cathedral. PhD thesis, Technical University of Catalonia, Spain. DOI:10.13140/RG.2.2.36194.94406

Elyamani, A. & Roca, P. (2018a). A review on the study of historical structures using integrated investigation activities for seismic safety assessment. Part I: dynamic investigation, *SCIENTIFIC CULTURE*, 4 (1), pp. 1-27, DOI: 10.5281/zenodo.1048241.

Elyamani, A. & Roca, P. (2018b). A review on the study of historical structures using integrated investigation activities for seismic safety assessment. Part II: model updating and seismic analysis, *SCIENTIFIC CULTURE*, 4 (1), pp. 29-51, DOI: 10.5281/zenodo.1048241.

Elyamani, A (2018). Re-use proposals and structural analysis of historical palaces in Egypt: the case of baron Empain palace in Cairo, *SCIENTIFIC CULTURE*, 4 (1), pp. 53-73. DOI: 10.5281/zenodo.1048245.

Elyamani, A., El-Rashidy, M. S., Abdel-Hafez, M., & Gad El-Rab, H. (2018b). A contribution to the conservation of 20th century architectural heritage in Khedival Cairo. *International Journal of Conservation Science*, 9(1), pp. 55-70.

El-Derby, A. A. O. D. & Elyamani, A. (2016). The adobe barrel vaulted structures in ancient Egypt: a study of two case studies for conservation purposes. *Mediterranean Archaeology and Archaeometry*, 16(1), pp. 295-315. DOI:10.5281/zenodo.46361.

Elyamani, A. (2016). Conservation-oriented structural analysis of the spire of Barcelona cathedral. *International Journal of Materials Science and Applications*, 5(6-2), 1-9. DOI: 10.11648/j.ijmsa.s.2016050602.11.

Elyamani, A. (2009). Wind and earthquake analysis of spire of cimborio of Barcelona cathedral. MSc thesis, Technical university of Catalonia, Barclona.Spain. DOI: 10.13140/RG.2.2.19492.17283.

Iervolino I, Galasso C, Cosenza E (2010) REXEL: computer aided record selection for code-based seismic structural analysis. *Bulletin of Earthquake Engineering*, 8:339-362. DOI: https://doi.org/10.1007/s10518-009-9146-1

Lourenço, P. B., Trujillo, A., Mendes, N. & Ramos, L. F. (2012). Seismic performance of the St. George of the Latins church: Lessons learned from studying masonry ruins. *Engineering structures*, 40, 501-518. DOI: https://doi.org/10.1016/j.engstruct.2012.03.003.

Martínez G (2007) Seismic vulnerability for middle and long span masonry historical buildings. PhD thesis, Technical University of Catalonia, Barcelona, Spain (in Spanish).

Mendes, N. (2012). Seismic assessment of ancient masonry buildings: shaking table tests and numerical analysis. PhD Thesis, University of Minho, Portugal.

Newmark, N. M. (1959). A method of computation for structural dynamics. In Proc. ASCE (Vol. 85, No. 3, pp. 67-94).

NCSE-02 (2002) Norma de construcción sismo resistente – Parte general y edificación. (In Spanish)

Peña, F., Lourenço, P. B., Mendes, N. & Oliveira, D. V. (2010). Numerical models for the seismic assessment of an old masonry tower. *Engineering Structures*, 32(5), 1466-1478. https://doi.org/10.1016/j.engstruct.2010.01.027.

Pereira, A. S. (2009). The opportunity of a disaster: the economic impact of the 1755 Lisbon earthquake. *The Journal of Economic History*, 69(02), 466-499.

SeismoArtif Ltd (2016) SeismoArtif V.2.1.: Software applications for generating artificial earthquake accelerograms, Pavia, Italy.

Trujillo, A. (2009). Stability analysis of Famagusta Churches: Saint George of the Latins. MSc Thesis, University of Minho, Portugal.